



Structural hot-spot stress approach for toe cracking from plate edge of load-carrying welded attachment

Takeshi Hanji¹ · Kazuo Tateishi¹ · Nima Rabsel¹ · Masaru Shimizu¹

Received: 27 July 2023 / Accepted: 10 February 2024 / Published online: 17 February 2024
© International Institute of Welding 2024

Abstract

The structural hot-spot stress approach is an effective method for assessing welding details when nominal stress is hard to determine due to geometric or loading complexities. Hot spots can be classified into two types: type “a,” which refers to a weld toe located on a plate surface, and type “b,” denoting one located on a plate edge. Previous studies on type “b” hot spots have mainly focused on in-plane gusset welded joints, and the applicability of type “b” hot-spot S-N curves proposed for in-plane gusset joints in IIW to the other details is not well understood. In this study, fatigue tests were conducted with a load-carrying attachment welded on a plate surface, where a crack occurred from a weld toe on the plate edge. The tests were also numerically simulated using finite element analysis. Upon evaluating the test results through the nominal stress, structural hot-spot stress (4, 8, and 12 mm method), and notch stress approaches, it was found that all the data lie above FAT71 for nominal stress, FAT100 for hot-spot stress, and FAT225 for effective notch stress.

Keywords Local stress · Type “b” hot spots · Load-carrying welded attachment

1 Introduction

Fatigue failure is a complex and progressive form of local damage caused by repetitive loads. Its severity is significantly influenced by both the magnitude of the load and the number of cycles. In steel bridges, fatigue cracks are mostly caused by secondary stresses resulting from the imposition of deformations. These stresses, not accounted for in the general design phase, can lead to what is known as distortion-induced fatigue [1]. Fatigue cracks usually occur at welded joints due to high stress concentration and residual tensile stress introduced by the welding process. To maintain and manage steel bridges rationally and strategically, accurate evaluation of the fatigue strength of welded joints under complex real-world behavior is crucial.

The most common method for evaluating fatigue strength in welded joints is the nominal stress approach [2], also referred to as the global approach. The global approach does

not account for the stress-raising effect due to welding and structural discontinuities and can even struggle to calculate nominal stress in cases with complex loading conditions or complicated geometry. Methods that do consider the local stress-raising effect have therefore been introduced and are referred to as local approaches.

The structural hot-spot stress approach is a local approach that is effective for assessing welding details when nominal stress is hard to determine due to geometric or loading complexities [2, 3]. The term “hot spot” refers to a critical location in structures where fatigue cracks are most likely to occur. Generally, the weld toe is considered to be a hot spot and can be classified into two types: type “a” refers to a weld toe located on a plate surface, while type “b” is that located on a plate edge.

Structural hot-spot stress accounts for the stress-raising effect due to the detail geometry but not the local notch effect caused by the shape of the weld. This approach was originally developed for welded tubular joints in offshore structures and was widely used in fatigue assessments in the 1960s [3, 4]. Later, in the early 1990s, the concept of hot-spot stress was extended to all kinds of plate structures. In welded structures, it has been suggested that the hot-spot stress approach is more suitable when the nominal stress is difficult to define due to complicated geometry or

Recommended for publication by Commission XIII - Fatigue of Welded Components and Structures

✉ Takeshi Hanji
hanji@civil.nagoya-u.ac.jp

¹ Nagoya University, Nagoya, Aichi, Japan

when structural discontinuity cannot be compared with classified details included in the design standards [5]. Progress has been made in the application of this approach, particularly in determining hot-spot stress via extrapolation methods based on two or three reference points [5], the structural stress approach by Dong [6], and the one-millimeter approach by Xiao and Yamada [7]. With the introduction and implementation of finite element analysis, the use of the structural hot-spot stress approach is gaining prominence, and most past studies have primarily focused on Type “a” hot spots.

As for type “b” hot spots, which involve cracks occurring from the plate edge, reference points for extrapolation methods cannot be defined as a function of plate thickness, as is the case with type “a” hot spots. Although there are various welded details with type “b” hot spots, past studies have mainly focused on in-plane gusset welded joints. Three extrapolation points at fixed distances of 4, 8, and 12 mm from the weld toe at the plate edge have been defined for determining type “b” hot-spot stress [8]. Currently, the International Institute of Welding (IIW) recommends two fatigue classes for in-plane gusset details featuring fatigue cracking from Type “b” hot-spots, depending on the attachment length. FAT100 applies to joints with short edge attachments (less than 100 mm), while FAT90 is for those with long edge attachments (more than 100 mm) [3].

Recently, some fatigue tests focusing on a fillet weld around a plate corner have been performed with cruciform joints, in which a fatigue crack occurred at the plate edge [9, 10]. The test results based on the structural hot-spot stress obtained by quadratic extrapolation over reference points 4, 8, and 12 mm have indicated the fatigue strength of 128.7 N/mm² at 2 million cycles and reasonable scatter band lying above the fatigue class of FAT100 [10]. On the other hand, other fatigue test results should be further accumulated to investigate whether type “b” hot-spot S-N curves proposed for in-plane gusset welded joints in IIW are applicable to other details with various geometries.

In this study, fatigue tests were conducted with a load-carrying attachment welded on a plate surface, where a crack originated from a weld toe on the plate edge (type “b” hot spot). The applicability of the recommended structural hot-spot S-N curves in IIW was examined based on both experimental and numerical results.

2 Fatigue tests

Fatigue tests were conducted by applying a tensile cyclic load to a load-carrying attachment welded on a plate surface. The test aimed to clarify cracking behavior and fatigue life.

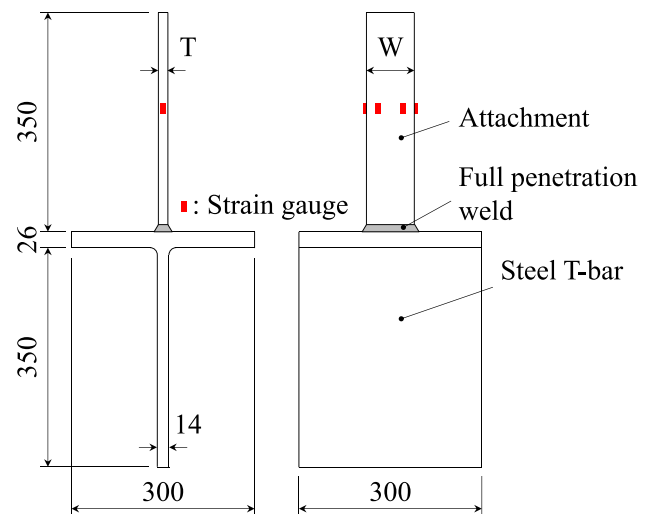


Fig. 1 Specimen (units: mm)

Table 1 Test cases

Specimen name	W (mm)	T (mm)
W80T6	80	6
W80T12	80	12
W80T25	80	25
W120T12	120	12
W160T6	160	6
W160T12	160	12

2.1 Specimens

The configurations and dimensions of the specimens are shown in Fig. 1 and Table 1. Each specimen consists of an attachment welded to the flange of a steel T-bar. Six different types of specimens, varying in attachment width and thickness, were used for the fatigue tests. Structural steel with a static strength of 400 N/mm² class was used for the attachments.

A K-groove was machined at the attachment end, and the attachment was connected to the steel T-bar with complete joint penetration welding. Gas metal arc welding with CO₂ shielding gas was used to fabricate the specimens. In specimen fabrication, first, the attachment was fixed to the steel T-bar using full penetration welding with a multi-pass weld. This was followed by boxing welding at both plate edges, overlapping the full penetration weld.

Weld profiles consisting of weld leg lengths, weld toe radius, and angle at the attachment side were measured for each specimen. Weld leg lengths were determined using a replica method in which silicon replicas of boxing weld beads were sliced and the profile of each sample

was subsequently measured by image analysis. A laser displacement sensor was used to measure the toe radius and angle around the corner of the attachment. During the laser measurement, the edge radius at the corner of the attachment was also measured.

The measurement results are summarized in Table 2. Note that there is no result for specimen W120T12 due to missing data. Similar weld leg lengths, toe radii, and angles were achieved across the specimen series. It was also observed that the corner of the attachment has a radius of curvature of about 0.4 mm on average.

2.2 Loading method

The experimental setup for the tests is shown in Fig. 2. Both the upper and lower sides of the specimen (attachment and web of steel T-bar sides) were secured in the testing machine, and a cyclic tensile load was applied to the specimen. The test was performed under a pulsating load with constant stress amplitude. The stress ratio was 0.05 for all specimens. The frequency of sinusoidal loading ranged from 1.4 to 6.0 Hz.

As shown in Fig. 1, strain gauges were affixed to the attachment surface to confirm the nominal stress range during the test. To detect crack initiation, copper wires were installed perpendicular to the weld toe at the attachment edge and corner. If the copper wire broke due to crack initiation, the loading process was automatically stopped. For some specimens, a beach mark test was performed to record the crack front on a fracture surface after confirming crack initiation. The fatigue life of the specimen was defined as the number of cycles until a crack from the attachment edge extended to at least half of the attachment width. If no crack was found on the specimen even after 5 million cycles, the result was recorded as a “runout” data point.

2.3 Fatigue crack observations

As shown in Fig. 3, beach mark observations of the fracture surface and magnetic particle tests confirmed that all the cracks originated from the weld toe at the attachment corner



Fig. 2 Experimental setup

and propagated as edge cracks. In a 25-mm-thick specimen (W80T25), an unexpected surface crack was observed at the weld toe in the flange of the steel T-bar, and loading was stopped upon its detection.

2.4 Fatigue strength evaluation based on nominal stress

Figure 4 shows the relationship between the nominal stress range and the fatigue life of each specimen. The nominal stress range was calculated by dividing the applied tensile load range by the sectional area of the attachment. In the graph, the fatigue strength curves for the as-welded state

Table 2 Weld profile measurements

Specimen name	Leg length (mm)		Toe radius (mm)	Toe angle (°)	Edge radius (mm)
	Attachment side	Steel T-bar side			
W80T6	13.1	8.7	2.4	46.0	0.4
W80T12	14.8	8.4	1.6	40.3	0.3
W80T25	17.4	9.4	1.7	36.4	0.4
W160T6	11.9	9.2	1.6	41.8	0.4
W160T12	13.6	9.1	1.6	33.6	0.4

Note: There is no result for specimen W120T12 due to missing data

Fig. 3 Fatigue cracking behavior

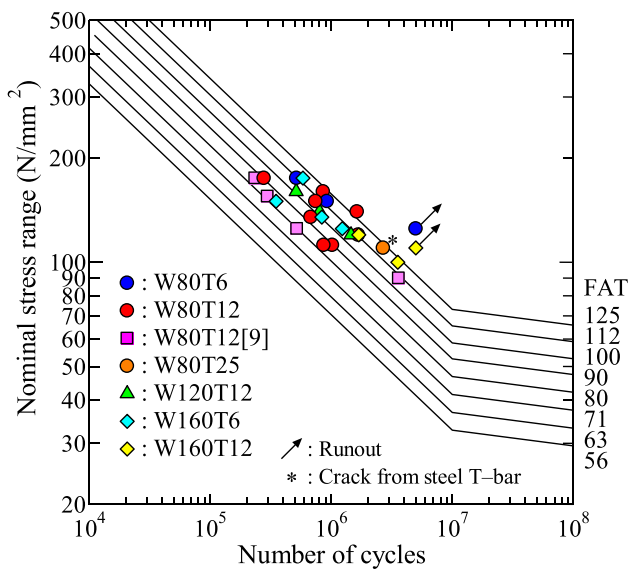
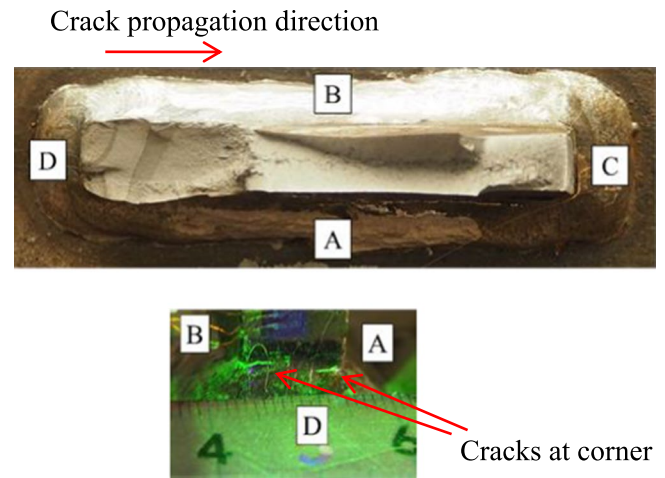


Fig. 4 Fatigue test results (nominal stress)

specified by IIW [1] are also shown. Specimens that failed due to cracking from the steel T-bar side are represented by an asterisk, and those that did not fail before 5 million cycles are indicated by an arrow. The graph also includes fatigue test results from similar specimens, where the width and thickness of the attachment were 80 mm and 12 mm, respectively [9].

According to the standard fatigue resistance S-N curves given in EN 1993 [11], the fatigue strength of this joint type varies depending on the thickness of the load-carrying plate and intermediate plate, as well as the weld size. It is recommended that a detail category of 71, meaning that the fatigue strength at 2 million cycles is 71 N/mm^2 , be applied to the specimen used in this study. Although the experimental results vary widely and the size effect of the attachment cannot be definitively confirmed, the lower limits for

all results are found to be distributed above the FAT71 curve as per IIW.

3 Application of local stress approach

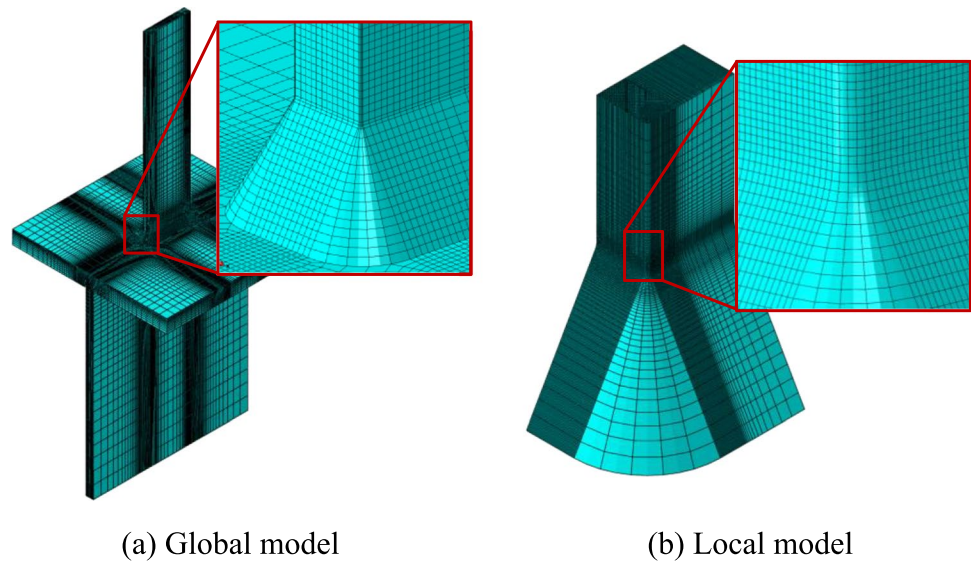
Finite element analysis (FEA) was used to calculate the local stress at the weld toe of the attachment edge for the specimen used in the fatigue tests, and the fatigue life of the specimen was evaluated using structural hot-spot stress and notch stress.

3.1 Finite element modeling

Along with the experiments, finite element analysis was conducted for all test specimens using Abaqus 6.14. Linear elastic analysis was carried out in two stages using global and local models through a sub-modeling technique. As shown in Fig. 5, the local model focuses only on the hot-spot region, i.e., around the weld toe of the attachment. Three-dimensional 20-node solid elements with a full integration point (C3D20) were used for all analyses. An elastic modulus of 200 kN/mm^2 and a Poisson's ratio of 0.3 were applied to both models.

In the global model, a minimum element size of 1 mm was used around the weld toe which satisfies the requirements ($\leq 4 \text{ mm} \times 4 \text{ mm}$) in IIW [3] and coarser meshes for the remaining parts of the model. The weld leg length measured in the specimen was incorporated into the model. The plate corner of the attachment was modeled to be rounded [10], and its radius was given as the average value of the measurements taken from the specimen, as summarized in Table 2. The boundary conditions were the same as the conditions under which the specimen was installed in the testing machine, and the load was applied to the end of the attachment to achieve a similar stress distribution to that measured by strain gauges on the specimen. Since bending

Fig. 5 Finite element model



deformation was slightly observed in the strain measurement on the attachment, a small bending load was applied to the model in addition to an axial load.

In the local model, a node-based sub-modeling technique was employed, in which the displacement fields obtained by the global model were applied as boundary conditions. The minimum element size of 0.1 mm was used in the local model. The weld toe radius and angle measured in the specimen were considered at the weld toe.

3.2 Stress distribution

Figure 6 shows an example of the maximum principal stress distribution obtained by the global and local models. From the analysis results, it was revealed that the highest stress concentration occurred at the weld toe of the attachment corner for all specimens, regardless of the attachment width

and thickness. This outcome is consistent with the cracking sites observed in the specimens.

3.3 Fatigue strength evaluation based on structural hot-spot stress

Figure 7 shows the relationship between the hot-spot stress range, as computed from FEA with the global model for each specimen, and the fatigue life as determined by the fatigue tests. The hot-spot stress range was identified on the cracked plate edge of the attachment using the 4, 8, and 12 mm method given in IIW [3]. The hot-spot stress shown in Fig. 7a was calculated from the stress distribution along the center of the plate thickness, while that in Fig. 7b was calculated from the stress distribution along the plate corner.

The results shown in Fig. 7b tend to be higher than those in Fig. 7a, suggesting that the hot-spot stress at the plate corner is slightly higher than that at the center of the

Fig. 6 Maximum principal stress distribution

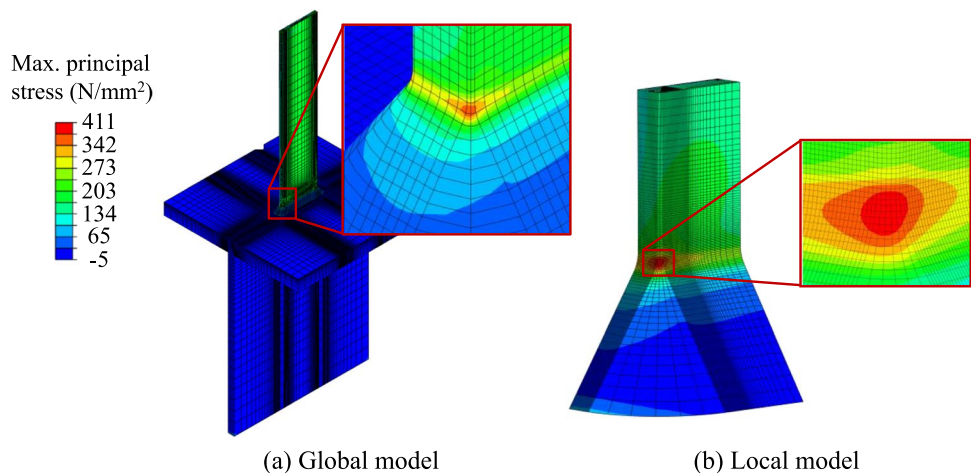
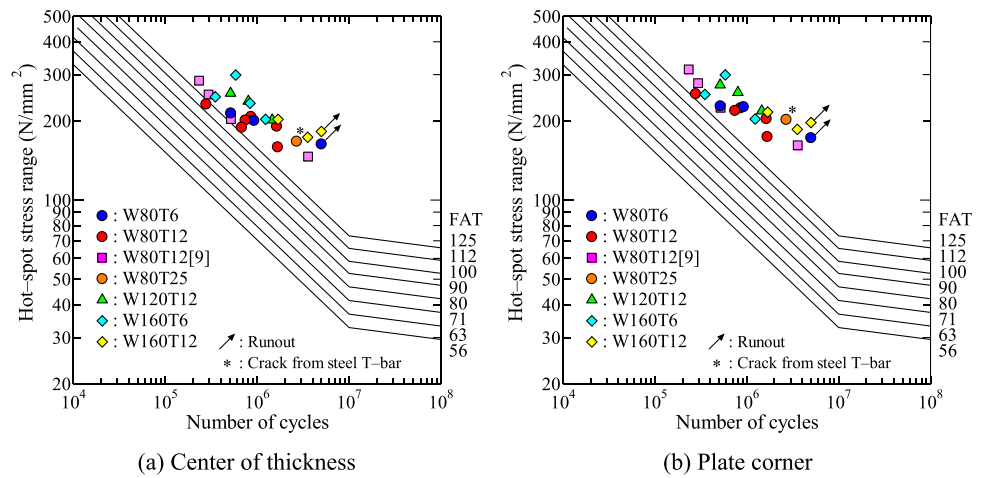


Fig. 7 Fatigue test results (hot-spot stress)



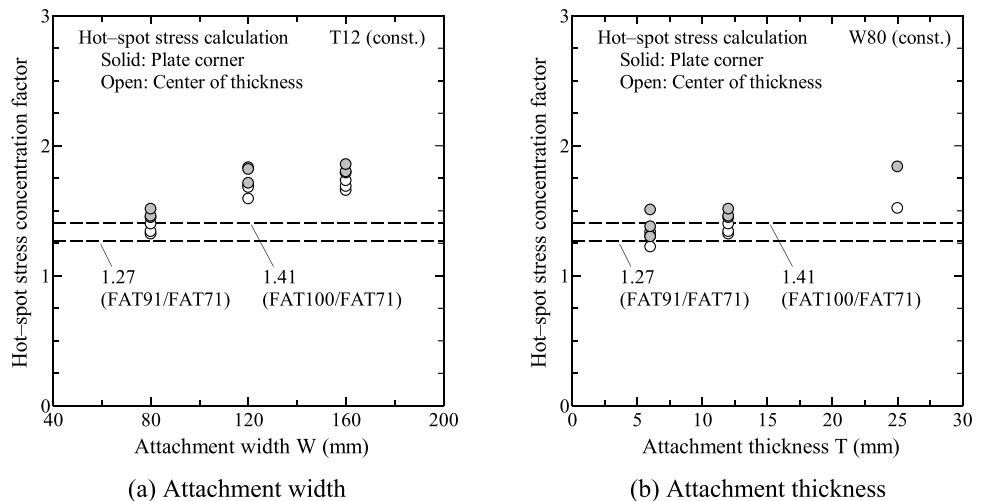
thickness. However, a similar degree of scattering can be found in both results. In both graphs, all the test results lie above FAT100, which is the type “b” hot-spot S-N curve proposed for in-plane gusset welded joints with a gusset length of less than 100 mm, as recommended by IIW. On the other hand, from Fig. 7b, FAT100 seems to give significantly conservative fatigue assessment for the corner crack in the specimen. This may be because the welding residual stress at the plate edge tends to be in compression [10], which may increase the fatigue strength of the specimen. Further investigation must be necessary to verify the fatigue class for the corner crack.

Figure 8 summarizes the structural stress concentration factor together with the attachment size. The stress concentration factor was obtained by dividing the hot-spot stress range by the nominal stress range. Regardless of the calculation location (plate corner or center of thickness), the stress concentration factor increases with increasing plate width and thickness.

3.4 Fatigue strength evaluation based on notch stress

The notch stress at the weld toe was obtained from the results for the local model. The relationship between the notch stress range and the fatigue life is shown in Fig. 9. The maximum principal stress at the weld toe was used as the notch stress. Generally, the local stress at the weld toe with a fictitious radius of 1 mm is used as the effective notch stress, and an S-N curve of FAT225 is recommended for all welded components, irrespective of the shape of the weld and joint, in the effective notch stress approach [12]. On the other hand, all specimens in this study tend to have a radius larger than 1 mm, so the toe radius for all local models was kept as the measured value for the specimens. As a result, all the results lie above FAT225, meaning that the effective notch stress is also effective in evaluating the fatigue strength of this joint detail with toe cracking from a plate edge, but the effective notch approach seems to result in overly conservative fatigue assessment for the corner crack

Fig. 8 Relationship between hot-spot stress concentration factor and attachment size



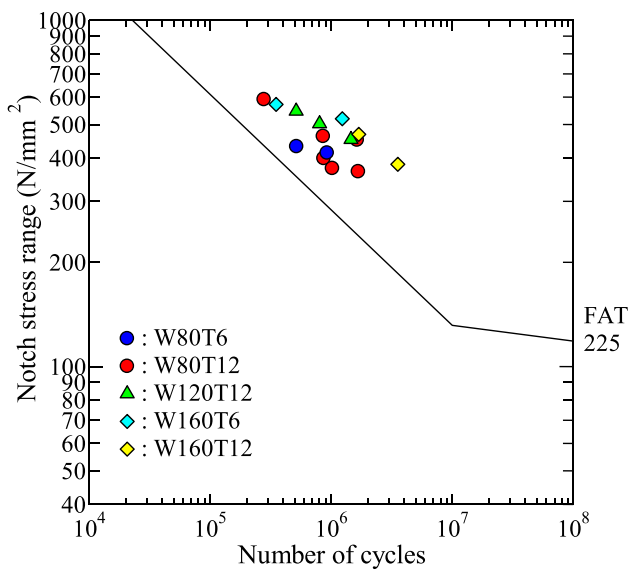


Fig. 9 Fatigue test results (notch stress using measured toe radii)

in the specimen. As mentioned above, this may be due to the welding residual stress at the plate edge in the specimen.

In this study, there was no significant difference in scatter bands of the result regardless of the cases of the nominal stress, structural hot-spot stress, and notch stress as shown in Figs. 4, 7, and 9. The reasons are considered to be that the structural stress concentration due to the attachment geometry did not differ significantly among the specimen series and that similar local geometry, such as the weld toe configuration and corner radius, strongly affecting the notch stress was achieved across the specimen series.

3.5 Size effect of attachment on local stress

The effect of the attachment size on the structural hot-spot stress and the notch stress was investigated via FEA, where

the width and thickness of the attachment were parametrically varied. The analysis was performed with the welded joints shown in Fig. 10, a slightly simplified version of the specimen used in the fatigue tests. In the model, different widths (W : 80, 120, 160, 200, 300, and 500 mm) and thicknesses (T : 12, 18, 25, 50, and 75 mm) of the attachment were considered.

The analysis procedure, including the element type and size, was kept the same as described in the previous section. In the global model, the bottom surface of the lower plate was fixed, and a load was applied to the end of the attachment. In the local model, the sub-modeling technique was adopted to save computational costs. A weld was modeled with equal leg lengths of 6 mm, and its toe configuration was set as a toe radius of 1 mm and a toe angle of 45° .

Figure 11 shows the distribution of the stress concentration factors for structural hot-spot stress and notch stress along the weld toe line. The horizontal axis represents the distance from the center of the thickness of the attachment edge, which is normalized by the attachment thickness T . In Fig. 11a, the plate thickness of the attachment remains constant at 25 mm, and its width varies from 80 to 500 mm, whereas in Fig. 11b, the thickness of the attachment is varied from 12 to 75 mm with a constant width of 160 mm.

The notch stress concentration factor (K_t) is at its maximum at the corner of the attachment, which corresponds to the crack initiation site in the experiment. Similarly, it can be confirmed that the hot-spot stress concentration factor (K_{hs}) varies in the thickness direction, with K_{hs} at the corner being slightly higher than that around the center of the thickness. In both cases, the peak stress concentration factors at the attachment corner increase as the attachment size becomes large.

Figure 12 shows the relationship between K_t at the attachment corner and K_{hs} . The relationship includes the K_{hs} values at both the corner and the center of the thickness of the attachment. Although there is a small thickness effect when

Fig. 10 Joint detail used in parametric FEA (units: mm)

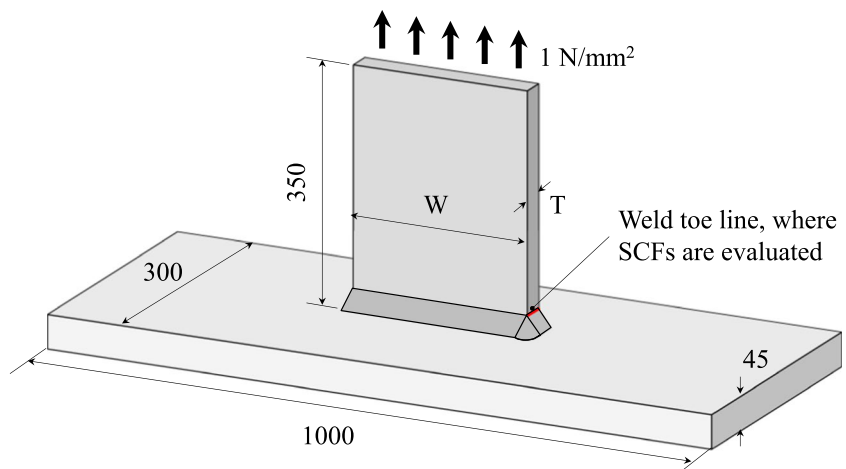


Fig. 11 Distributions of stress concentration factors along weld toe

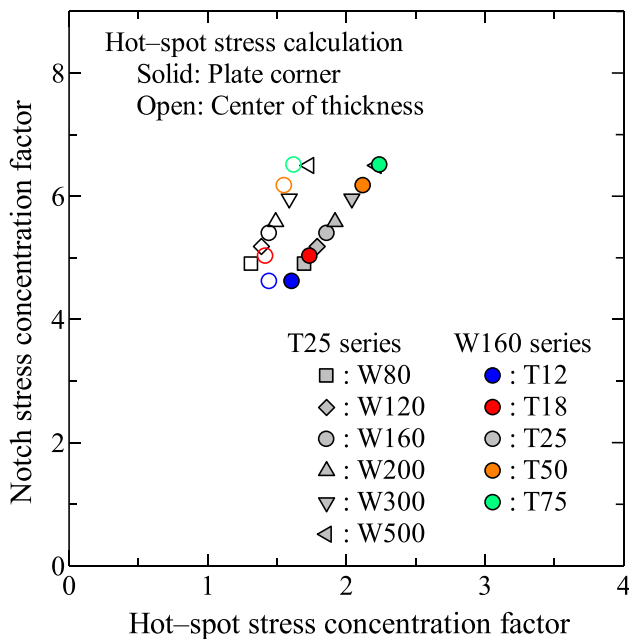
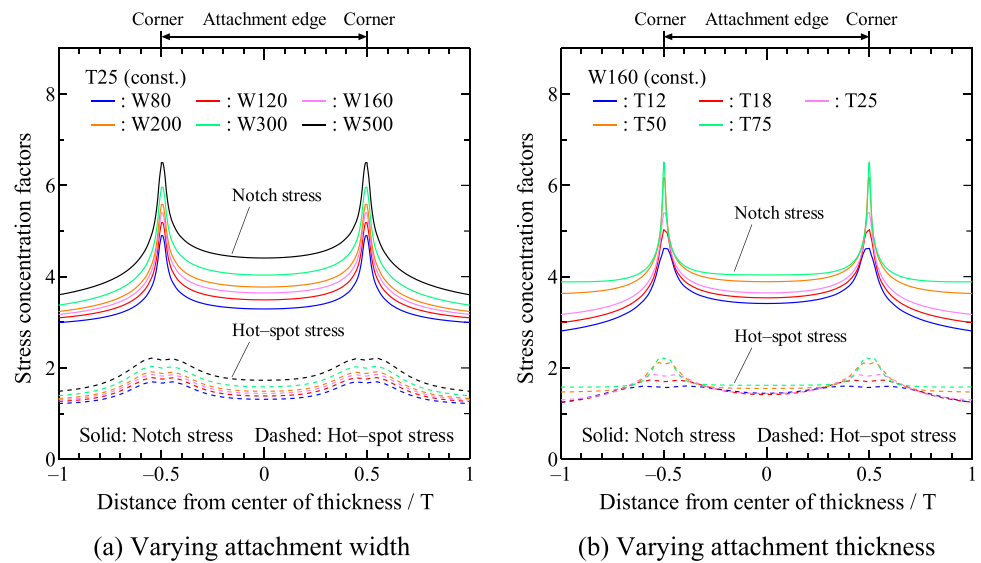


Fig. 12 Relationship between notch stress and hot-spot stress

calculating the hot-spot stress at the center of the thickness, relatively good correlations can be observed for both relationships, irrespective of the size of the attachment. This suggests that the structural hot-spot stress, determined by the 4, 8, and 12 mm method, can adequately capture the size effect of the attachment on the notch stress at the weld toe.

4 Conclusions

In this study, both experimental and numerical studies were conducted to investigate the applicability of the structural hot-spot stress approach to toe cracking for type “b” hot spots in a load-carrying welded attachment. The main conclusions drawn from this study are as follows:

- 1) The fatigue test confirmed that a crack originates from the weld toe at the attachment corner and propagates along the weld toe as an edge crack. This implies that the joint detail in this study exhibits toe cracking from the type “b” hot spot.
- 2) The fatigue strength for the specimen was evaluated using the nominal stress approach. The findings revealed that all data lie above FAT71 in the nominal stress case, which agrees with the recommendation given in EN 1993.
- 3) The test specimen was numerically simulated using finite element analysis. Both the structural hot-spot stress (4, 8, and 12 mm method) and the notch stress at the weld toe of the attachment edge were calculated for each specimen. Evaluation of the test results using structural hot-spot stress and notch stress approaches revealed that all the data lie above FAT100 in the hot-spot stress case and FAT225 in the effective notch stress case.
- 4) Both the structural hot-spot stress and notch stress increase with increasing width and thickness of the attachment.
- 5) A relatively good correlation exists between the structural hot-spot stress and the notch stress, regardless of the size of the attachment. This indicates that the structural hot-spot stress determined by the 4, 8, and 12 mm

method can adequately capture the effect of the attachment size on the notch stress at the weld toe.

Acknowledgements They would also like to express their sincere gratitude to Mr. Yoshimine at Nippon Sharyo, Ltd. for fabricating the specimens.

Funding The authors gratefully acknowledge the support provided by the Japan Society for the Promotion of Science (JSPS) KAKENHI (Grant Number 21K04233).

Declarations

Conflict of interest The authors declare no competing interests.

References

1. Fisher JW, Kulak GL, Smith IFC (1998) A fatigue primer for structural engineers. National Steel Bridge Alliance
2. Hobbacher AF (2016) Recommendations for fatigue design of welded joints and components, 2nd edn. Springer, Cham
3. Niemi E, Fricke W, Maddox SJ (2018) Structural hot-spot stress approach to fatigue analysis of welded components, designer's guide, 2nd ed. Springer Singapore
4. Marshall PW, Wardenier J (2005) Tubular versus non-tubular hot spot stress methods, Proceedings of the fifteenth international offshore and polar engineering conference, 254-263
5. Niemi E (1995) Stress determination for fatigue analysis of welded components. Woodhead Publishing
6. Dong P (2001) A structural stress definition and numerical implementation for fatigue analysis of welded joints. *Int J Fatigue* 23(10):865–876
7. Xiao ZG, Yamada K (2004) A method of determining geometric stress for fatigue strength evaluation of steel welded joints. *Int J Fatigue* 26(12):1277–1293
8. Niemi E (1994) On the determination of hot spot stresses in the vicinity of edge gussets, IIW documentation, XIII-1555-94
9. Saito F, Anami K, Ikehara I, Shibuya A, Ono S (2017) Fatigue strength improvement at attachment side boxer weld by low temperature transformation welding material. *J Struct Eng* 63A:681–689 (in Japanese)
10. Fricke W, Gao L, Paetzold H (2017) Fatigue assessment of local stresses at fillet welds around plate corners. *Int J Fatigue* 101(2):169–176
11. Nussbaumer A, Borges L, Davaine L (2018) Fatigue design of steel and composite structures, 2nd edn: Eurocode 3: Design of steel structures part 1-9 – Fatigue / Eurocode 4: Design of composite steel and concrete structures, ECCS
12. Fricke W (2012) IIW recommendations for the fatigue assessment of welded structures by notch stress analysis. Woodhead Publishing

Publisher's note Springer Nature remains neutral with regard to jurisdictional claims in published maps and institutional affiliations.

Springer Nature or its licensor (e.g. a society or other partner) holds exclusive rights to this article under a publishing agreement with the author(s) or other rightsholder(s); author self-archiving of the accepted manuscript version of this article is solely governed by the terms of such publishing agreement and applicable law.